



# The impact of Last Glacial climate variability in west-European loess revealed by radiocarbon dating of fossil earthworm granules

Olivier Moine, Pierre Antoine, Christine Hatté, Amaelle Landais, Jérôme Mathieu, Charlotte Prud'Homme, Denis-Didier Rousseau

## ► To cite this version:

Olivier Moine, Pierre Antoine, Christine Hatté, Amaelle Landais, Jérôme Mathieu, et al.. The impact of Last Glacial climate variability in west-European loess revealed by radiocarbon dating of fossil earthworm granules. *Proceedings of the National Academy of Sciences of the United States of America*, 2017, 114 (24), pp.6209-6214. 10.1073/pnas.1614751114 . hal-01606544

**HAL Id: hal-01606544**

**<https://hal.science/hal-01606544>**

Submitted on 26 May 2020

**HAL** is a multi-disciplinary open access archive for the deposit and dissemination of scientific research documents, whether they are published or not. The documents may come from teaching and research institutions in France or abroad, or from public or private research centers.

L'archive ouverte pluridisciplinaire **HAL**, est destinée au dépôt et à la diffusion de documents scientifiques de niveau recherche, publiés ou non, émanant des établissements d'enseignement et de recherche français ou étrangers, des laboratoires publics ou privés.



Distributed under a Creative Commons Attribution 4.0 International License



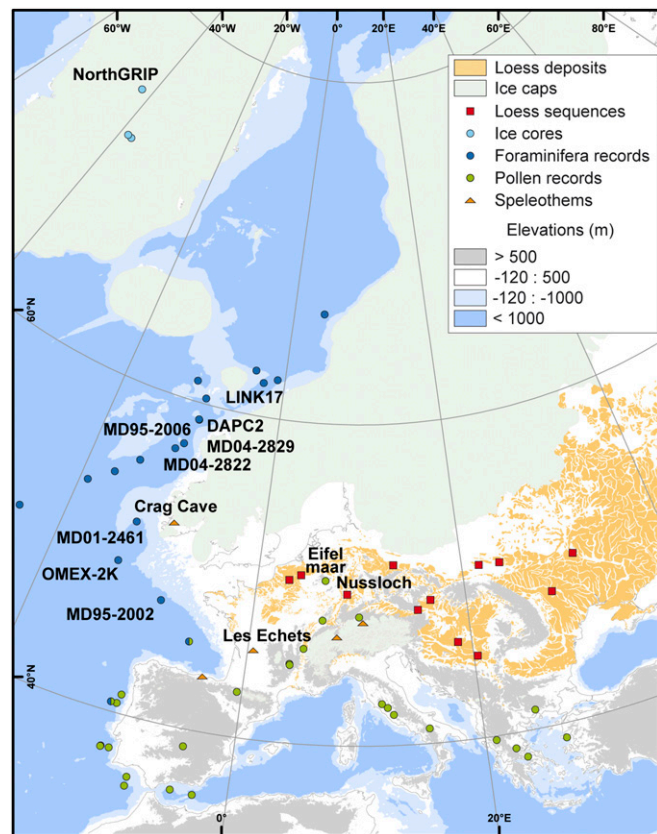


**Fig. 1.** Location of the Nussloch site in the European Loess Belt. Last Glacial records discussed in the text are named.

between the types of paleosols in the loess records and both duration and intensity of associated GI (16). However, limitations in absolute dating of loess sequences still inhibit the use of this type of terrestrial record for depicting regional climatic and environmental changes in association with GI. Archaeological layers aside, the scarcity of organic remains, such as wood, charcoal, and bone, results in a lack of reliable radiocarbon ages. Optically stimulated luminescence (OSL) methods ubiquitously used in loess do not solve this problem owing to their inherent 10% error margins. Poor chronological control weakens our proposed correlations and conceptual model linking loess–tundra gley alternations with GS–GI cycles (14, 17), which are based on (i) the succession pattern of both soil horizons and GI, (ii) the relative importance of the different events in both records, and (iii) correspondences between major variations of two Aeolian dynamic proxies [i.e., the loess grain size index and the Greenland ice core dust ( $\text{Ca}^{2+}$ ) concentration] (18). Despite its coherency, this correlation scheme remains partially debated (19) and still requires validation by a precise and accurate independent chronology.

## Results

Here, we present a consistent radiocarbon chronology of all Middle and Upper Pleniglacial paleosols of the Nussloch loess sequence from a promising radiocarbon dating methodology applied to earthworm calcite granules (Fig. 2), hereafter simply referred to as granules (*Methods*). Granules are scarce in loess units but very abundant in tundra gleys and arctic to boreal brown soils (20). Many factors render granules interesting and optimum for precise chronology: (i) granule carbon is mainly derived from feeding sources (i.e., litter), (ii) experiments on *Lumbricus terrestris* revealed a very low content in old or dead carbon from soils in granule  $\delta^{13}\text{C}$  (21), (iii) granules are mainly released at the soil surface (22), (iv) evidence of earthworm-induced

bioturbation is absent in tundra gleys and very rare in arctic to boreal brown soils according to both field and thin-section observations, and (v) the earthworm habitat is restricted to a depth of a few decimeters between the surface and the permafrost table in tundra gley horizons given the periglacial conditions essential to their formation, which is not necessarily the case in arctic to boreal brown soils that did not develop on permafrost. Taking into account all of these specificities, risks of age overestimation resulting from old carbon pollution and age underestimation caused by artificial time shifts between granules and sediment are strongly limited (more details are in *Methods*). The Nussloch site shows the most complete pedostratigraphic succession of Western Europe between 55 and 20 ka (14, 23) (Fig. S1). It is thus ideal for this application of granule radiocarbon dating in a loess context. We constructed a composite record including all pedostratigraphic units by stacking the upper 11.5 m of P4 profile on the lower 7 m of P8 profile (Fig. S2). All ages of soil horizons from P3, P4, and P8 profiles (Table S1) were then transposed onto the composite record (Fig. 3 and Fig. S2).

Calibrated ages range between 44,949–48,595 and 13,814–14,453 ka cal. B.P. (Table S1). Most of the  $2\sigma$  errors are of 0.6–2.5% (100–800 y) from 36 to 13 ka cal. B.P. and 1.9–3.7% (700–1,500 y) from 44 to 38 ka cal. B.P. and vary more largely between 3.9% (1,800 y) and 7.0% (3,300 y) approaching the age limit of radiocarbon dating. However, these uncertainties are significantly lower than those of luminescence ages and similar to those of the latest Greenland age model ranging from ~0.17 to ~2.3 ka for this time interval (24). Only two ages seem largely underestimated: the age from incipient gley 8b (IG8b) on P8 by 3.5 ka compared with its equivalent on P4, and the age from IG9b on P4 by 7 ka compared with that extrapolated from the sedimentation rate (Fig. 3 and Table S1). In their respective profiles, both are located about 1.5 m below the present day surface within a zone bioturbated by modern roots and earthworms (Fig. S1). We consider that these two samples are probably contaminated by postglacial to modern granules. With

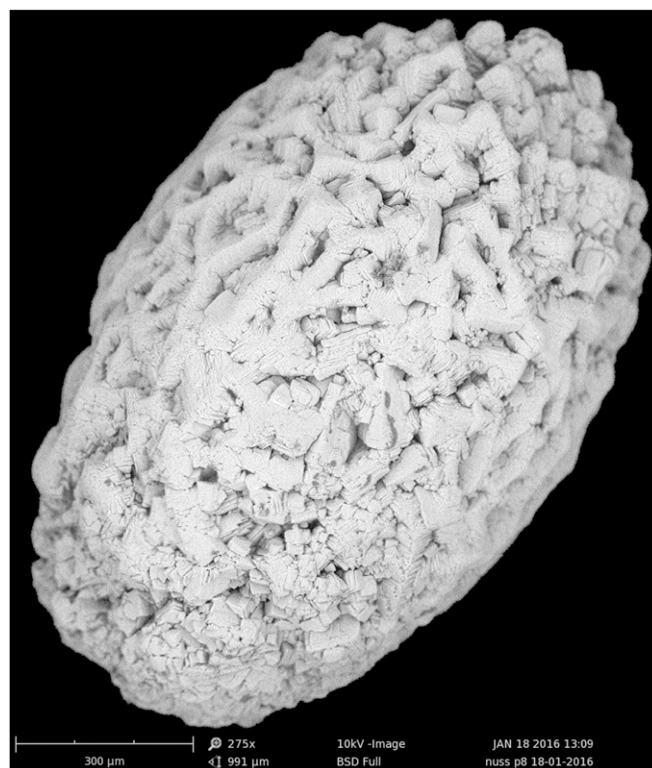


**Fig. 2.** Scanning electron microscope (SEM) view of a fossil carbonate granule of *Lumbricus* earthworm from the Nussloch P8 loess profile. BSD, backscattered electron detector. Modified from CoDEM/BATLAB.



the above two results discarded, all remaining ages define a chronological series with no statistically significant age inversion. Age reproducibility checks performed in tundra gley units Gm3 and G1a on P8 are positive (Fig. 3 and Table S1). Ages from arctic to boreal brown soils fit well among tundra gleys ages. Ages from tundra gleys Gm3 and Gm1, located only 40 cm below the base of the Lohne Soil and the Upper Gräselberg Soil, respectively, do not seem rejuvenated as one might expect if bioturbation related to these more developed soils was important (Table S1). In absence of deep earthworm activity in these permafrost-free paleosols, dated granules might have mainly been produced by epigeic earthworms living close to the soil surface rather than anecic earthworms that usually dig deep burrows (25). Reliable ages are thus obtained from all tundra gleys and arctic to boreal brown soils as long as they are not affected by deep bioturbations from the topsoil. The regular distribution of radiocarbon ages throughout the loess profile indicates an almost continuous sedimentation between 50 and 20 ka. Sedimentation rates derived for the 45- to 21-ka interval are higher in loess units than in pedogenetic horizons. They increase from 0.19 mm/y for the Middle Pleniglacial to 0.33 and 1.12 mm/y for the early and full Upper Pleniglacial, respectively (Fig. 3), matching previous estimates based on luminescence ages and previous correlations with Greenland (14). We can now confidently establish correlations with other archives over the entire Nussloch sequence and especially after 30 ka.

## Discussion

Two major changes in sedimentary and environmental dynamics are evidenced in the Nussloch loess sequence records. The first one around 30 ka presents a major limit marked by a sharp and strong increase in both sedimentation rate (Fig. 3) and grain size index (GSI) (14). These features observed in almost all of the loess sequences from Western to Eastern Europe (26–30) thus constitute a major marker level for stratigraphic correlations. This marker level at ~30 ka is, within limit uncertainties, synchronous with (i) a first step of expansion of the Last Glacial maximum (LGM) Fennoscandian ice sheet and mountain ice caps because of higher precipitations (31, 32), (ii) a significant drop in sea level from about –60 to –100 m (33), and (iii) a change from anastomosing to higher-energy braided channels in west European fluvial systems (34). This configuration induced a widening of deflation areas on the continental shelves of the North Sea and Channel and in large river valleys and a very strong increase in detrital particles available for Aeolian deflation and transport, enabling the deposition of markedly thicker loess units over Europe (35). A second marker level, observed around 23 ka at the top of tundra gley G7, is characterized by a sharp decrease in the GSI, an almost complete disappearance of the rich mollusk fauna of Nussloch (17), a shift from finely laminated to homogeneous loess in Western and Central Europe (26, 27, 30), and a significant increase in the sand content in Eastern Europe (28, 29). This marker level at ~23 ka, also recorded across the European Loess Belt, indicates a shift to markedly more arid conditions between 23 and 20 ka contemporaneous with maxima in ice sheet extension and volume. However, very low sea level and high-energy braided channels in the deflation areas persisted during this time interval, permitting high loess sedimentation rate (~1 mm/y) to be maintained in European loess profiles.

Furthermore, based on our radiocarbon chronology, reliable correlations between the pedostratigraphical sequence of Nussloch and Greenland climate proxy records over the 55- to 20-ka interval can now be established (Fig. 3). Each tundra gley and arctic to boreal brown soils correlates with a single GI within dating uncertainties (Methods). The only two exceptions are related to low sedimentation rates during the Middle Pleniglacial. The tundra gley Gm3, which is twice the thickness of Gm2 and Gm1, most likely stacks two successive tundra gleys formed during GI 11 and GI 10 (i.e., during the Hengelo interstadial) (36, 37). Similarly, the Lohne Soil appears likely as a stack of two soil horizons developed during GI 8 and GI 7c (i.e., during the initial phase of the Denekamp interstadial complex) (36). Our

chronology thus confirms and updates previous correlations (Table S2) based on Aeolian dynamic proxies. Around 50° N, Crag Cave speleothems (southwest Ireland) constitute the only other record of most Last Glacial interstadials. Indeed, their growth phases are induced by climate ameliorations contemporaneous to GI (38) as well as mollusk abundance increases in Nussloch soil horizons (17, 39). However, speleothem growth ceases during stadials, whereas loess deposition continues, hence revealing additional variability.

We can thus distinguish, within Nussloch loess units above tundra gley G4, eight additional slightly hydromorphic horizons with oxidized root tracks, hereafter called IGs, dated between about 27 and 21 ka (Fig. 3). By comparison with tundra gleys, IGs are thinner (only 10- to 15-cm thick) and have weaker iron redox imprints, implying a thinner permafrost active layer with lower ice content and weaker water release during the thawing season. Changes in mollusk assemblages recorded in IGs from Nussloch profile P3 also reflect weaker humidity increases as well as weaker or similar decreases in vegetation diversity but no appreciable warming phase (17) compared with tundra gleys. Likewise, magnetic properties of the sediment studied at high resolution throughout Nussloch profile P8 led to a similar conclusion (40). Although Nussloch tundra gleys are always associated with strong decreases in GSI and Greenland  $[Ca^{2+}]$  (14), it is not systematic for IGs (Fig. 4). Moreover, no significant  $\delta^{18}O$  increases in Greenland records can be identified in contemporaneous time intervals to IGs. The formation of these IGs may thus imply weaker precipitation increases and northward shifts of the Polar front than those leading to the formation of the main tundra gleys. The radiocarbon chronology established from the Nussloch loess sequence thus reveals a more complex pattern than identified until now within MIS 2 in Greenland  $\delta^{18}O$  records. Indeed, the unsuspected centennial environmental variability exhibited in the Nussloch loess record during MIS 2 shows that the LGM was probably not as stable as generally admitted.

Among records that display short and low-magnitude oscillations during MIS 2, one can cite for the North Atlantic Ocean those of *Neogloboquadrina pachyderma* (sinistral) percentages from the Rockall Trough (41, 42) (Fig. 1), the Cariaco Basin reflectance influenced by movements of the Intertropical Convergence Zone (43), and the Bermuda Rise calcium concentration influenced by the Atlantic Meridional Overturning Circulation (44) (Fig. 4). In Europe, both Les Echets Lake magnetic susceptibility (45) and Eifel maar varve thickness (46) were likely influenced by the Aeolian transport, and in China, the Qinghai Lake dust flux above 25  $\mu m$  was influenced by the Westerlies (47). The acquisition of more high-resolution and well-dated terrestrial and marine records is thus required to thoroughly evaluate the significance of both IGs and minor LGM oscillations. Additional development of coupled modeling experiments will be necessary to improve our understanding of associated climate mechanisms and interactions.

Future applications of this radiocarbon dating strategy based on earthworm calcite granules will improve correlations between loess sequences. This fundamental step forward will contribute to build a well-dated reference environmental framework across the European Loess Belt for the study of late Neanderthal and early Anatomically Modern Human peopling of Europe and their interactions with climate and environmental changes.

## Methods

**The Choice of Earthworm Calcite Granules for Radiocarbon Dating.** West European Last Glacial loess sequences generally lack organic remains, such as wood, charcoals, and bones, which are required for radiocarbon dating. In this area, only particular geomorphological structures, like the Nussloch thermokarst infillings (19, 23) (Fig. S1 and Table S1), or archeological levels, may provide these materials that only exceptionally yield long-term coherent chronologies as, for example, in Central Europe (48, 49). A ubiquitous carbon-bearing material should thus be identified. To address the issue of a detailed chronology for the Last Glacial, the dating of loess bulk organic matter has been used throughout the Nussloch loess sequence (50). Despite a better precision than for OSL ages, these results show age underestimations

High-resolution counts recently undertaken throughout French Upper Weichselian loess sequences revealed very high *Lumbricus* granule abundances in tundra gley horizons and arctic brown soils (several hundred per 10 L of





SEM photographs of earthworm calcite granule. This study was supported by Grant ANR-08-BLAN-0227 from Agence Nationale de la Recherche (to D.-D.R., P.A., C.H. and O.M.), by a project from CNRS "Projets Exploratoires Premier

Soutien" program (to P.A. and O.M.), and by CNRS ARTEMIS calls for  $^{14}\text{C}$  dating (to O.M., P.A. and C.H.). This paper is LDEO contribution no. 8109 and LSCE contribution no. 6161.

- Dansgaard W, et al. (1993) Evidence for general instability of past climate from a 250-kyr ice-core record. *Nature* 364:218–220.
- Sánchez Goñi MF, Harrison SP (2010) Millennial-scale climate variability and vegetation changes during the Last Glacial: Concepts and terminology. *Quat Sci Rev* 29:2823–2827.
- Rasmussen TL, Thomsen E, Moros M (2016) North Atlantic warming during Dansgaard-Oeschger events synchronous with Antarctic warming and out-of-phase with Greenland climate. *Sci Rep* 6:20535.
- Baldini JUL, Brown RJ, McElwaine JN (2015) Was millennial scale climate change during the Last Glacial triggered by explosive volcanism? *Sci Rep* 5:17442.
- Zhang X, Lohmann G, Knorr G, Purcell C (2014) Abrupt glacial climate shifts controlled by ice sheet changes. *Nature* 512:290–294.
- Flückiger J, Knutti R, White JWC, Renssen H (2008) Modeled seasonality of glacial abrupt climate events. *Clim Dyn* 31:633–645.
- Rhodes RH, et al. (2015) Paleoclimate. Enhanced tropical methane production in response to iceberg discharge in the North Atlantic. *Science* 348:1016–1019.
- Guillevic M, et al. (2014) Evidence for a three-phase sequence during Heinrich Stadial 4 using a multiproxy approach based on Greenland ice core records. *Quat Sci Rev* 106:167–185.
- Fletcher WJ, et al. (2010) Millennial-scale variability during the last glacial in vegetation records from Europe. *Quat Sci Rev* 29:2839–2864.
- Luetscher M, et al. (2015) North Atlantic storm track changes during the Last Glacial Maximum recorded by Alpine speleothems. *Nat Commun* 6:6344.
- Moreno A, et al. (2014) A compilation of Western European terrestrial records 60–8 ka BP: Towards an understanding of latitudinal climatic gradients. *Quat Sci Rev* 106:167–185.
- Haase D, et al. (2007) Loess in Europe—its spatial distribution based on a European Loess Map, scale 1:2,500,000. *Quat Sci Rev* 26:1301–1312.
- Frechen M, Oches EA, Kohfeld KE (2003) Loess in Europe—mass accumulation rates during the Last Glacial period. *Quat Sci Rev* 22:1835–1857.
- Antoine P, et al. (2009) Rapid and cyclic aeolian deposition during the Last Glacial in European loess: A high-resolution record from Nussloch, Germany. *Quat Sci Rev* 28:2955–2973.
- Rousseau D-D, Derbyshire E, Antoine P, Hatté C (2007) Loess records. Europe. *Encyclopedia of Quaternary Science*, ed Elias SA (Elsevier, Amsterdam), pp 1440–1456.
- Rousseau D-D, et al. (2007) Link between European and North Atlantic abrupt climate changes over the last glaciation. *Geophys Res Lett* 34:L22713.
- Moine O, Rousseau D-D, Antoine P (2008) The impact of Dansgaard-Oeschger cycles on the loessic environment and malacofauna of Nussloch (Germany) during the Upper Weichselian. *Quat Res* 70:91–104.
- Rousseau D-D, et al. (2002) Abrupt millennial climatic changes from Nussloch (Germany) Upper Weichselian eolian records during the Last Glaciation. *Quat Sci Rev* 21:1577–1582.
- Kadereit A, Kind C-J, Wagner GA (2013) The chronological position of the Lohne Soil in the Nussloch loess section – re-evaluation for a European loess-marker horizon. *Quat Sci Rev* 59:67–86.
- Prud'homme C, et al. (2015) Earthworm calcite granules: A new tracker of millennial-timescale environmental changes in Last Glacial loess deposits. *J Quat Sci* 30:529–536.
- Canti MG (2009) Experiments on the origin of  $^{13}\text{C}$  in the calcium carbonate granules produced by the earthworm *Lumbricus terrestris*. *Soil Biol Biochem* 41:2588–2592.
- Canti M, Pearce TG (2003) Morphology and dynamics of calcium carbonate granules produced by different earthworm species. *Pedobiologia (Jena)* 47:511–521.
- Antoine P, et al. (2001) High-resolution record of the last interglacial-glacial cycle in the Nussloch loess-paleosol sequences, Upper Rhine Area, Germany. *Quat Int* 76-77:211–229.
- Rasmussen SO, et al. (2014) A stratigraphic framework for abrupt climatic changes during the Last Glacial period based on three synchronized Greenland ice-core records: Refining and extending the INTIMATE event stratigraphy. *Quat Sci Rev* 106:14–28.
- Rundgren S (1975) Vertical distribution of lumbricids in southern Sweden. *Oikos* 26:299–306.
- Antoine P, et al. (2013) High-resolution record of the environmental response to climatic variations during the Last Interglacial–Glacial cycle in Central Europe: The loess-paleosol sequence of Dolní Věstonice (Czech Republic). *Quat Sci Rev* 67:17–38.
- Antoine P, et al. (2016) Upper Pleistocene loess-paleosol records from Northern France in the European context: Environmental background and dating of the Middle Palaeolithic. *Quat Int* 411:4–24.
- Haesaerts P, et al. (2003) The East Carpathian loess record: A reference for the Middle and Late Pleniglacial stratigraphy in Central Europe. *Quaternaire* 14:163–188.
- Rousseau D-D, et al. (2011) North Atlantic abrupt climatic events of the last glacial period recorded in Ukrainian loess deposits. *Clim Past* 7:221–234.
- Meszner S, Kreutzer S, Fuchs M, Faust D (2013) Late Pleistocene landscape dynamics in Saxony, Germany: Paleoenvironmental reconstruction using loess-paleosol sequences. *Quat Int* 296:97–104.
- Hughes AC, et al. (2016) The last Eurasian ice sheets – a chronological database and time-slice reconstruction, DATED-1. *Boreas* 45:1–45.
- Ivy-Ochs S, et al. (2008) Chronology of the last glacial cycle in the European Alps. *J Quat Sci* 23:559–573.
- Clark PU, et al. (2009) The last glacial maximum. *Science* 325:710–714.
- Vandenberghe J (2003) Climate forcing of fluvial system development: An evolution of ideas. *Quat Sci Rev* 22:2053–2060.
- Sima A, et al. (2009) Imprint of North-Atlantic abrupt climate changes on western European loess deposits as viewed in a dust emission model. *Quat Sci Rev* 28:2851–2866.
- Puzachenko AY, et al. (2016) The Eurasian mammoth distribution during the second half of the Late Pleistocene and the Holocene: Regional aspects. *Quat Int*, 10.1016/j.quaint.2016.05.019.
- Vandenberghe J, van der Plicht J (2016) The age of the Hengelo interstadial revisited. *Quat Geochronol* 32:21–28.
- Fankhauser A, McDermott F, Fleitmann D (2016) Episodic speleothem deposition tracks the terrestrial impact of millennial-scale last glacial climate variability in SW Ireland. *Quat Sci Rev* 152:104–117.
- Moine O, Rousseau D-D, Antoine P (2005) Terrestrial molluscan records of Weichselian Lower to Middle Pleniglacial climatic changes from the Nussloch loess series (Rhine Valley, Germany): The impact of local factors. *Boreas* 34:363–380.
- Taylor SN, Lacroix F (2015) Magnetic anisotropy reveals the depositional and post-depositional history of a loess-paleosol sequence at Nussloch (Germany). *J Geophys Res Solid Earth* 120:2859–2876.
- Austin WEN, et al. (2012) The synchronization of palaeoclimatic events in the North Atlantic region during Greenland Stadial 3 (ca 27.5 to 23.3 kyr b2k). *Quat Sci Rev* 36:154–163.
- Scourse JD, et al. (2009) Growth, dynamics and deglaciation of the last British–Irish ice sheet: The deep-sea ice-rafted detritus record. *Quat Sci Rev* 28:3066–3084.
- Deplazes G, et al. (2013) Links between tropical rainfall and North Atlantic climate during the last glacial period. *Nat Geosci* 6:213–217.
- Henry LG, et al. (2016) North Atlantic ocean circulation and abrupt climate change during the last glaciation. *Science* 353:470–474.
- Wohlfarth B, et al. (2008) Rapid ecosystem response to abrupt climate changes during the last glacial period in western Europe, 40–16 ka. *Geology* 36:407–410.
- Sirocko F, et al. (2016) The ELSA-Vegetation-Stack: Reconstruction of Landscape Evolution Zones (LEZ) from laminated Eifel maar sediments of the last 60,000 years. *Global Planet Change* 142:108–135.
- An Z, et al. (2012) Interplay between the Westerlies and Asian monsoon recorded in Lake Qinghai sediments since 32 ka. *Sci Rep* 2:619.
- Haesaerts P, et al. (2010) Charcoal and wood remains for radiocarbon dating Upper Pleistocene loess sequences in Eastern Europe and Central Siberia. *Palaeogeogr Palaeoclimatol Palaeoecol* 291:106–127.
- Nigst PR, et al. (2014) Early modern human settlement of Europe north of the Alps occurred 43,500 years ago in a cold steppe-type environment. *Proc Natl Acad Sci USA* 111:14394–14399.
- Hatté C, Pessenda L-C, Lang A, Paterne M (2001) Development of accurate and reliable  $^{14}\text{C}$  chronologies for loess deposits: Application to the loess sequence of Nussloch (Rhine valley, Germany). *Radiocarbon* 43:611–618.
- Hatté C, Morvan J, Noury C, Paterne M (2001) Is classical Acid-Alkali-Acid treatment responsible for contamination? An alternative proposition. *Radiocarbon* 43:177–182.
- Lang A, et al. (2003) High-resolution chronologies for loess: Comparing AMS  $^{14}\text{C}$  and optical dating results. *Quat Sci Rev* 22:953–959.
- Bibus E, Frechen M, Kösel M, Rähle W (2007) Das jungpleistozäne Lößprofil von Nußloch (SW-Wand) im Aufschluss der Heidelberger Zement AG. *Eiszeitalt Gegenw* 56:227–255.
- Tissoux H, et al. (2010) OSL and ESR studies of Aeolian quartz from the Upper Pleistocene loess sequence of Nussloch (Germany). *Quat Geochronol* 5:131–136.
- Gocke M, et al. (2014) Introducing an improved multi-proxy approach for paleoenvironmental reconstruction of loess–paleosol archives applied on the Late Pleistocene Nussloch sequence (SW Germany). *Palaeogeogr Palaeoclimatol Palaeoecol* 410:300–315.
- Zöller L, Stremme H, Wagner GA (1988) Thermolumineszenz-datierung an Löss-Paläoboden-Sequenzen von Nieder-, Mittel- und Oberrhein/Bundesrepublik Deutschland. *Chem Geol* 73:39–62.
- Evin J, Maréchal J, Pachiaudi C, Puisségur J-J (1980) Conditions involved in dating terrestrial shells. *Radiocarbon* 22:545–555.
- Frechen M, Terhorst B, Rähle W (2007) The Upper Pleistocene loess/paleosol sequence from Schatthausen in North Baden-Württemberg. *Eiszeitalt Gegenw* 56:212–227.
- Schirmer W (2012) Rhine loess at Schwalbenberg II – MIS 4 and 3. *E&G Quat Sci J* 61:32–47.
- Goßfriend GA, Stipp JJ (1983) Limestone and the problem of radiocarbon dating of land-snail shell carbonate. *Geology* 11:575–577.
- Pigati JS, Rech JA, Nekola JC (2010) Radiocarbon dating of small terrestrial gastropod shells in North America. *Quat Geochronol* 5:519–532.
- Pustovoytov K, Terhorst B (2004) An isotopic study of late Quaternary loess-paleosol sequence in SW Germany. *Rev Mex Cienc Geol* 21:88–93.
- Canti M (1998) Origin of calcium carbonate granules found in buried soils and Quaternary deposits. *Boreas* 27:275–288.
- Hodson ME, et al. (2015) Biomineralisation by earthworms – an investigation into the stability and distribution of amorphous calcium carbonate. *Geochim Trans* 16:4.
- Antoine P (2012) Données stratigraphiques et sédimentologiques. *Quaternaire* 5:13–19.
- Canti M, Bronk-Ramsey C, Hua Q, Marshall P (2015) Chronometry of pedogenic and stratigraphic events from calcite produced by earthworms. *Quat Geochronol* 28:96–102.
- Tisnérat-Laborde N, Poupeau J-J, Tannau J-F, Paterne M (2001) Development of a semi-automated system for routine preparation of carbonate samples. *Radiocarbon* 43:299–304.
- Cottéreau E, et al. (2007) Artemis, the new  $^{14}\text{C}$  AMS at LMC14 in Saclay, France. *Radiocarbon* 49:291–299.
- Czernik J, Goslar T (2001) Preparation of graphite targets in the Gliwice Radiocarbon Laboratory for AMS  $^{14}\text{C}$  dating. *Radiocarbon* 43:283–291.
- Goslar T, Czernik J, Goslar E (2004) Low-energy  $^{14}\text{C}$  AMS in Poznań Radiocarbon Laboratory, Poland. *Nucl Instrum Methods Phys Res B* 223:224:5–11.
- Reimer PJ, et al. (2013) IntCal13 and Marine13 radiocarbon age calibration curves 0–50,000 years cal BP. *Radiocarbon* 55:1869–1887.